PHYSICAL REVIEW E **76**, 035303(R) (2007)

Dynamical effects and phase separation in cooled binary fluid films

Lennon Ó Náraigh and Jean-Luc Thiffeault*
Department of Mathematics, Imperial College, London SW7 2AZ, United Kingdom
(Received 13 March 2007; revised manuscript received 26 July 2007; published 21 September 2007)

We study phase separation in thin films using a model based on the Navier-Stokes Cahn-Hilliard equations in the lubrication approximation, with a van der Waals potential to account for substrate-film interactions. We solve the resulting thin-film equations numerically and compare to experimental data. The model captures the qualitative features of real phase-separating fluids, in particular, how concentration gradients produce film thinning and surface roughening. The ultimate outcome of the phase separation depends strongly on the dynamical back reaction of concentration gradients on the flow, an effect we demonstrate by applying a shear stress at the film's surface. When the back reaction is small, the phase domain boundaries align with the direction of the imposed stress, while for larger back-reaction strengths, the domains align in the perpendicular direction.

DOI: 10.1103/PhysRevE.76.035303 PACS number(s): 47.15.gm, 47.55.−t, 64.75.+g

When a binary fluid is cooled below the critical temperature, the mixed state is energetically unfavorable and the system spontaneously phase separates and forms domains rich in either fluid component [1,2]. Due to the relevance of phase-separating thin films in industrial applications [3], many experiments and numerical simulations focus on understanding how phase separation is altered if the binary fluid forms a thin layer on a substrate. To explain the main features of these studies, we propose a lubrication approximation of the coupled Navier-Stokes Cahn-Hilliard equations for a thin layer of fluid with a free surface.

Several recent experiments have clarified the different regimes of domain growth in a binary thin film. Wang and Composto [4] have identified early, intermediate, and late stages of evolution. The early stage comprises three-dimensional domain growth, while the intermediate stage is characterized by the formation of wetting layers at the film boundaries, the thinning of the middle layer, and significant surface roughening. Due to the thinning of the middle layer, the sandwichlike structure breaks up, and matter from the wetting layer flows back into the bulk. Thus, a late stage is reached, consisting of bubbles coated by thin wetting layers. This characterization of the evolution has been seen in other experiments [5,6], although clearly a variety of behaviors is possible, depending on the wetting properties of the mixture. Our model captures the essential features of this evolution, in particular the tendency for concentration gradients to promote film rupture and surface roughening.

In a series of papers, Das *et al.* [7,8] numerically investigate the behavior of binary fluids with wetting. In [7] they study the wetting properties of a binary mixture in an ultrathin film. The behavior is different from that in bulk mixtures. In bulk mixtures, where one component of the binary fluid is preferentially attracted to the boundary, a layer rich in this component is established at the boundary, followed by a depletion layer. This layered structure propagates into the bulk and is called a spinodal wave [8]. In ultrathin films, where the film thickness is less than a spinodal wavelength, this layered structure is suppressed. Two types of behavior are then possible. In the partially wet case, both fluid components come into contact with the film boundaries. The ultimate state of the system is a domainlike structure extending in the lateral directions. The domains grow in time as $t^{1/3}$, indicating Lifshitz-Slyozov diffusion [9]. In the other case, complete wetting, only one of the fluid components is in contact with the film boundaries. Our focus in this paper is on the partially wet case.

The papers of Das *et al.* elucidate the roles of wetting and film thickness in phase separation, although they do not discuss hydrodynamics or the effect of free-surface variations on domain formation. Here, we therefore focus on ultrathin films with a variable free surface, and for simplicity we restrict our attention to the case where both fluids experience the same interaction with the substrate and free surface. The model we introduce is based on the Navier-Stokes Cahn-Hilliard equations [10]. With an applied external forcing, the model highlights the effect of the dynamical back reaction of concentration gradients on the flow, a useful feature in applications where control of phase separation is required [11].

In full generality, the equations we study are

$$\frac{\partial \boldsymbol{v}}{\partial t} + \boldsymbol{v}\cdot\boldsymbol{\nabla}\boldsymbol{v} = \boldsymbol{\nabla}\cdot\boldsymbol{T} - \frac{1}{\rho}\boldsymbol{\nabla}\phi, \tag{1a}$$

$$\frac{\partial c}{\partial t} + \boldsymbol{v}\cdot\boldsymbol{\nabla}c = D\nabla^2(c^3 - c - \gamma\nabla^2 c), \tag{1b}$$

$$\boldsymbol{\nabla}\cdot\boldsymbol{v} = 0, \tag{1c}$$

where

$$T_{ij} = -\frac{p}{\rho}\delta_{ij} + \nu\left(\frac{\partial v_i}{\partial x_j} + \frac{\partial v_j}{\partial x_i}\right) - \beta\gamma\frac{\partial c}{\partial x_i}\frac{\partial c}{\partial x_j} \tag{1d}$$

is the stress tensor, p is the fluid pressure, ϕ is the body force potential, and ρ is the constant density. Additionally, ν is the kinematic viscosity, β is the mixture free energy per unit mass, D is the Cahn-Hilliard diffusion coefficient, and $\sqrt{\gamma}$ is the thickness of domain boundaries. The concentration

*Present address: Department of Mathematics, University of Wisconsin, Madison, WI 53706, USA. jeanluc@mailaps.org

boundary condition for Eq. (1) is $\boldsymbol{n}\cdot\boldsymbol{\nabla}c=\boldsymbol{n}\cdot\boldsymbol{\nabla}(\nabla^2 c)=0$, where $\boldsymbol{n}$ is a vector normal to the boundary, while the boundary conditions on the velocity and stress tensor are standard [12]. We nondimensionalize these equations by using the vertical length scale h_0, the horizontal or lateral length scale λ, and the diffusion time λ^2/D. If the parameter $\varepsilon=h_0/\lambda$ is small, a lubrication approximation is possible [12]. We take the following dimensionless groups to be of order unity:

$$\mathrm{Re}=\frac{\varepsilon D}{\nu}, \qquad C=\frac{\rho\nu D}{h_0\sigma_0\varepsilon^2},$$

$$r=\frac{\varepsilon^2\beta\gamma}{D\nu}, \qquad C_n=\frac{\varepsilon\sqrt{\gamma}}{h_0},$$

where Re is the Reynolds number, C_n is the Cahn number [10] which provides a dimensionless measure of domain wall thickness, r is a dimensionless measure of the back-reaction strength, and C^{-1} is a dimensionless measure of surface tension determined by the reference-level dimensional surface tension σ_0. Using these scalings, we expand the nondimensional version of Eq. (1) in powers of ε, following the method outlined in [12], and obtain equations for the free surface height $h(x,y,t)$ and concentration $c(x,y,t)$,

$$\frac{\partial h}{\partial t}+\boldsymbol{\nabla}_\perp\cdot(\boldsymbol{u}h)=0, \tag{2a}$$

$$\frac{\partial}{\partial t}(ch)+\boldsymbol{\nabla}_\perp\cdot(\boldsymbol{u}ch)=\boldsymbol{\nabla}_\perp\cdot(h\boldsymbol{\nabla}_\perp\mu), \tag{2b}$$

where

$$\boldsymbol{u}=\frac{1}{2}h\boldsymbol{\nabla}_\perp\sigma-\frac{1}{3}h^2\left[\boldsymbol{\nabla}_\perp\left(-\frac{1}{C}\boldsymbol{\nabla}_\perp^2 h+\phi\right)+\frac{r}{h}\boldsymbol{\nabla}_\perp(h|\boldsymbol{\nabla}_\perp c|^2)\right],$$

$$\mu=c^3-c-C_n^2\frac{1}{h}\boldsymbol{\nabla}_\perp\cdot(h\boldsymbol{\nabla}_\perp c).$$

Here $\boldsymbol{\nabla}_\perp=(\partial_x,\partial_y)$ is the gradient operator in the lateral directions, $\boldsymbol{u}$ is the vertically averaged velocity, σ is the dimensionless, spatially varying surface tension, and ϕ is the body force potential. The first term in the equation for $\boldsymbol{u}$ comes from the boundary condition on T_{ij} on the free surface [12]. While the equations do not allow for vertical variations in concentration, we show in what follows that the model reproduces the qualitative features observed in thin binary fluids, especially in the case where both binary fluid components interact identically with the substrate and free surface [7].

For thin films with $h_0=100-1000$ nm [4,5], the dominant contribution to the potential is due to van der Waals interactions [12,13], and following these references we take $\phi=Ah^{-3}$, where A is the dimensionless Hamaker coefficient. To prevent rupture [12], we study films where $A<0$, and take A to be independent of the concentration level, so that both binary fluid components are attracted equally to the substrate and free surface boundaries. In this case, Eq. (2) possesses simple one-dimensional equilibrium solutions, obtained by setting $\boldsymbol{u}=\boldsymbol{\nabla}_\perp\mu=0$. From Fig. 1 we see that the one-dimensional equilibrium solution of Eq. (2), with boundary conditions $h(\pm\infty)=1$, $c(\pm\infty)=\pm1$, consists of a steplike profile for the concentration, corresponding to a pair of domains separated by a smooth transition region. Across this transition region, the height field dips into a valley. While the valley increases in depth for large backreaction strength r, the film never ruptures. This result follows from the inequality $h''(0)>0$, since $x=0$ is a local minimum. Thus, at equilibrium,

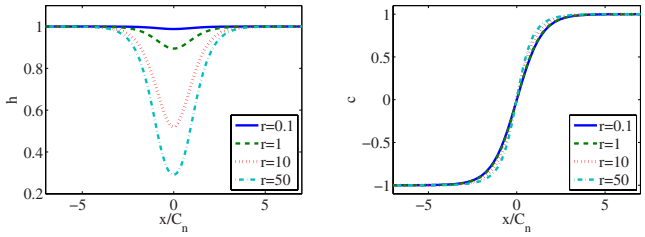

(a) (b)

FIG. 1. (Color online) Equilibrium solutions of Eq. (2) for $C=C_n^2=|A|=1$ and $r=0.1,1,10,50$. In (a) the valley deepens with increasing r although the film never ruptures, while in (b) the front steepens with increasing r.

$$0<\left[1+\frac{r}{C_n^2|A|}\left(\frac{1}{4}(c(0)^2-1)^2+\frac{1}{2}C_n^2c'(0)^2\right)\right]^{-1}<[h(0)]^3.$$

In this way, the repulsive van der Waals potential has a regularizing effect on the solutions.

Physically, the formation of the valley arises from the balance between the van der Waals and back-reaction effects. From the solution in Fig. 1, the capillary force $F_{\mathrm{cap}}=-rh^{-1}\partial_x[h(\partial_x c)^2]$ and the van der Waals force $F_{\mathrm{vdW}}=|A|\partial_x h^{-3}$ always have opposite signs. The repulsive van der Waals force acts as a nonlinear diffusion [14] and inhibits rupture, and therefore F_{cap} promotes rupture, a result seen in experiments [4]. The valley in the height field represents a balance between the smoothening and the rupture-inducing effects.

As in ordinary Cahn-Hilliard dynamics [2], the one-dimensional equilibrium solution hints at the late-time state in higher dimensions. Thus, we expect the multidimensional solution to comprise concentration domains with a height field of peaks and valleys, with valleys occurring at domain boundaries. Numerical simulations show that this is indeed the case. Our study of domain size uses an average wave number (k_x,k_y), obtained from the Fourier transform of the correlation function $\langle c(\boldsymbol{x},t)c(\boldsymbol{x}+\boldsymbol{r},t)\rangle$ [15]. Using this definition, we find that the domains grow in time as $t^{1/3}$, the usual Lifshitz-Slyozov growth law [9]. Here $\boldsymbol{x}=(x,y)$ denotes the lateral coordinates and $\langle\cdots\rangle$ denotes the spatial average. The modified growth exponent due to hydrodynamic effects [2,16] is not observed, since the diffusive time scale determines the asymptotic ordering in the derivation of Eq. (2). The surface roughness arising from the concentration gradients is similar to that observed in the one-dimensional case and has been seen in several experiments [4,18].

Although the effect of hydrodynamics is not important for domain growth, the coupling of concentration gradients to

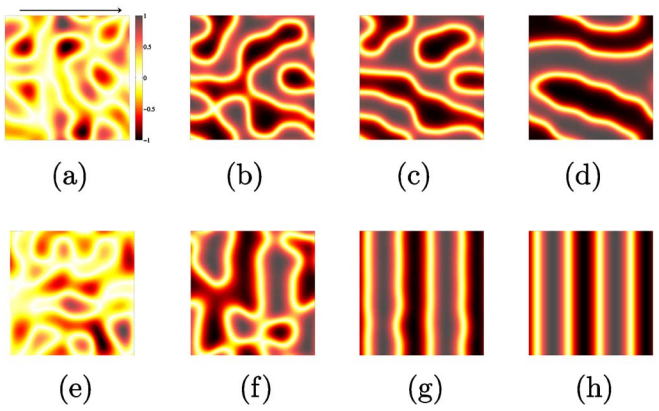

FIG. 2. (Color online) Concentration field for $C=1$, $A=-10$. Across the first row, $r=0$ and $t=$ (a) 1000; (b) 3750; (c) 7500; (d) 30 000. Across the second row, $r=1/4$ and $t=$ (e) 1000; (f) 3750; (g) 7500; (h) 30 000. The surface tension gradient is parallel to the arrow, and $\sigma=\Sigma_0 \sin(kx)$, $\Sigma_0=20$, and $k=4k_0$. In (a)–(d) with $r=0$, the domains align along the arrow, while in (e)–(h) with moderate back-reaction strength, the domains align in a direction perpendicular to the arrow.

the flow is the origin of the back reaction in our equations. The resulting interplay of free-surface height and concentration variations has dramatic effects on the phase separation when we apply a surface tension gradient across the film. Physically, this can be realized by differential heating of the surface [19], although a surfactant will also induce stresses at the surface [20]. We set $\sigma=\Sigma_0 \sin kx$, where Σ_0 is a dimensionless amplitude, $k=(2\pi/L)m=k_0 m$ is the spatial scale of the surface tension variation, and m is an integer. Then the velocity that drives the system becomes

$$\boldsymbol{u} = \frac{1}{2}h(k\Sigma_0 \cos kx, 0) + \frac{1}{3}h^2\left[\boldsymbol{\nabla}_\perp\left(\frac{1}{C}\nabla_\perp^2 h + \frac{|A|}{h^3}\right) - \frac{r}{h}\boldsymbol{\nabla}_\perp(h|\nabla_\perp c|^2)\right].$$

This velocity field may also be obtained by imposing a shear stress $\boldsymbol{\tau}$ at the surface, with $\boldsymbol{\tau}=\boldsymbol{\nabla}_\perp\sigma$ [21]. We carry out simulations with this forcing on a 128×128 grid. The results do not change upon increasing the resolution. The parameter C_n is chosen to regularize domain boundaries [17]. The other parameter values are indicated in the caption to Fig. 2.

This choice of velocity field leads to control of phase separation in the following manner. For small values of the backreaction strength, with $r\to0$, the height field quickly aligns with the surface tension profile as in Fig. 3, since the strong effect of the van der Waals diffusion destroys the unforced part of $h(\boldsymbol{x},t)$. At the same time, the concentration field begins to form domains. At later times, when $k_x(t), k_y(t)\sim k$, the domains align with the gradient of the forcing term. The growth of the domains continues in this direction and is arrested (or slowed down considerably) in the direction perpendicular to the forcing. The domains are stringlike, with kinks occurring along lines where $\sigma(x,y)$ is minimized, as evidenced by Figs. 2(a)–2(d). The time dependence of the average wave number (k_x,k_y) is shown in Fig. 4. It is not clear whether the decay of (k_x,k_y) is arrested or continues slowly, and we do not report the decay rate here.

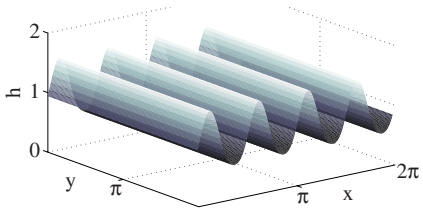

FIG. 3. (Color online) Height field for $r=0$ and $t=30\,000$ aligns with the applied surface tension. The height field at $t=30\,000$ for $r=1/4$ is similar.

For moderate values of the back-reaction strength with $r\sim O(1)$, the height field again assumes a profile aligned with the surface tension, while domains of concentration now align in a direction perpendicular to the forcing gradient. Domain growth continues in the perpendicular direction and is arrested in the direction of the driving-force gradient. A pattern of stringlike domains emerges, with domain boundaries forming along lines where both $\sigma(x,y)$ and $h(x,y,t)$ are maximized. Eventually, the domain boundaries align perfectly with the surface tension maxima, as evidenced in Figs. 2(e) and 2(h).

The control of phase separation by surface shear therefore depends crucially on the back reaction. This result is amplified by the existence of a no-rupture condition only for the $r=0$ case (no back reaction). This condition relies on the alignment of the height and surface tension profiles, which is exact only when the back reaction is zero. Then, at late times, the system evolves towards equilibrium and is described by the steady state $\boldsymbol{\nabla}_\perp\cdot\left[\frac{1}{2}h^2\boldsymbol{\nabla}_\perp\sigma+\frac{1}{3}h^3\boldsymbol{\nabla}_\perp(C^{-1}\nabla_\perp^2 h+|A|h^{-3})\right]=0$, which by the alignment property reduces to the one-dimensional equation

$$h^2\left[\frac{1}{2}\frac{d\sigma}{dx}+\frac{1}{3}h\frac{d}{dx}\left(\frac{1}{C}\frac{d^2h}{dx^2}+\frac{|A|}{h^3}\right)\right]=\text{const.}$$

By multiplying both sides of the expression by h, differentiating, and then evaluating the result at x_0, a minimum of both surface tension and height, we obtain the condition

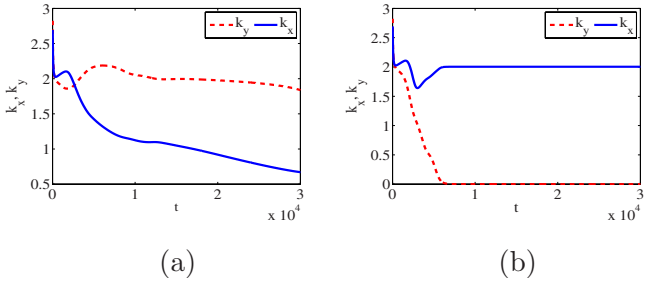

FIG. 4. (Color online) Time dependence of k_x and k_y for (a) $r=0$, where the secular behavior of k_x and k_y has a small drift whose rate we do not report; (b) $r=1/4$, where $k_x\to2$ and $k_y\to0$.

$$[h(x_0)]^3\left(\frac{1}{3C}h(x_0)h^{(4)}(x_0)+\frac{1}{2}k^2\Sigma_0\right)=|A|h''(x_0). \qquad (3)$$

Since x_0 is a minimum of height, $h''(x_0)>0$, which prevents $h(x_0)$ from being zero. On the other hand, for r and Σ_0 sufficiently large, the alignment of height and surface tension profiles is not exact, the one-dimensional state is never reached, and hence the result in Eq. (3) does not apply. In that case, simulations show that the film ruptures in finite time.

Given an applied surface tension gradient, we have outlined, by numerical simulations and calculations, three possible outcomes for the phase separation, depending on the back-reaction strength r. For $r\ll 1$, the concentration forms stringlike domains, aligned with the applied force. For $r\sim O(1)$, the concentration forms domains aligned perpendicular to the applied force. For $r\gg 1$, the forcing causes the film to rupture. Thus, in a real fluid, the interfacial tension or back reaction must be tuned to achieve the desired outcome.

In conclusion, we have derived a thin-film model of phase separation based on the Navier-Stokes Cahn-Hilliard equations, in which the reaction of concentration gradients on the flow is important. We have used this model to give a qualitative picture of phase separation in thin films, in particular the tendency of concentration gradients to promote rupture, and to produce peaks and valleys in the free surface that mirror the underlying domain morphology. In the presence of a unidirectional sinusoidal variation in surface tension, the strength of the back reaction determines the direction in which the domains align. This result could prove useful in microfabrication applications where control of phase separation is required [11].

Because the lubrication model suppresses vertical variations in the concentration field, we are limited to the case where the binary fluid components interact identically with the substrate and free surface. However, the model quite generally gives an accurate description of surface roughening arising from van der Waals forces. More detailed models based on this approach, involving different boundary conditions that better reflect wetting behavior [7,22] and a concentration-dependent Hamaker coefficient, can capture a wider range of thin-film behavior.

L.O.N. was supported by the Irish government and the U.K. Engineering and Physical Sciences Research Council. J.-L.T. was supported in part by the U.K. EPSRC Grant No. GR/S72931/01.

[1] J. W. Cahn and J. E. Hilliard, J. Chem. Phys. **28**, 258 (1957); J. Zhu, L. Q. Shen, J. Shen, and V. Tikare, Phys. Rev. E **60**, 3564 (1999).

[2] A. J. Bray, Adv. Phys. **43**, 357 (1994).

[3] A. Karim, J. F. Douglas, L. P. Sung, and B. D. Ermi, in *Encyclopedia of Materials: Science and Technology*, edited by K. H. Jürgen Buschow, Robert W. Cahn, Merton C. Flemings, Bernard Ilschner, Edward J. Kramer, Subhash Mahajan, and Patrick Veyssière (Elsevier, Amsterdam, 2002); D. L. Smith, *Thin-Film Deposition: Principles and Practice* (McGraw-Hill, New York, 1995); K. Mertens, V. Putkaradze, D. Xia, and S. R. Brueck, J. Appl. Phys. **98**, 034309 (2005).

[4] H. Wang and R. J. Composto, J. Chem. Phys. **113**, 10386 (2000).

[5] H. J. Chung and R. J. Composto, Phys. Rev. Lett. **92**, 185704 (2004).

[6] W. Wang, T. Shiwaku, and T. Hashimoto, Macromolecules **36**, 8088 (2003); H. Hoppe, M. Heuberger, and J. Klein, Phys. Rev. Lett. **86**, 4863 (2001).

[7] S. K. Das, S. Puri, J. Horbach, and K. Binder, Phys. Rev. E **72**, 061603 (2005).

[8] S. Puri and K. Binder, Phys. Rev. E **66**, 061602 (2002); , Phys. Rev. Lett. **86**, 1797 (2001); S. Puri, K. Binder, and H. L. Frisch, Phys. Rev. E **56**, 6991 (1997).

[9] I. M. Lifshitz and V. V. Slyozov, J. Phys. Chem. Solids **19**, 35–50 (1961).

[10] J. Lowengrub and L. Truskinowsky, Proc. R. Soc. London, Ser. A **454**, 2617 (1998).

[11] G. Krausch, E. J. Kramer, M. H. Rafailovich, and J. Sokolov, Appl. Phys. Lett. **64**, 2655 (1994).

[12] A. Oron, S. H. Davis, and S. G. Bankoff, Rev. Mod. Phys. **69**, 931 (1997).

[13] V. A. Parsegian, *Van der Waals Forces* (Cambridge University Press, New York, 2001).

[14] R. S. Laugesen and M. C. Pugh, Electron. J. Differ. Equations **2002**, 1 (2002).

[15] L. Ó Náraigh and J.-L. Thiffeault, Phys. Rev. E **75**, 016216 (2007).

[16] S. Berti, G. Boffetta, M. Cencini, and A. Vulpiani, Phys. Rev. Lett. **95**, 224501 (2005).

[17] L. Berthier, J.-L. Barrat, and J. Kurchan, Phys. Rev. Lett. **86**, 2014 (2001); , Eur. Phys. J. B **11**, 635 (1999).

[18] K. D. Jandt, J. Heier, F. S. Bates, and E. J. Kramer, Langmuir **12**, 3716 (1996).

[19] A. P. Krekhov and L. Kramer, Phys. Rev. E **70**, 061801 (2004); N. Garnier, R. O. Grigoriev, and M. F. Schatz, Phys. Rev. Lett. **91**, 054501 (2003).

[20] A. E. Hosoi and J. W. M. Bush, J. Fluid Mech. **442**, 217 (2001).

[21] T. G. Myers, J. P. F. Charpin, and C. P. Thompson, Phys. Fluids **14**, 240 (2001).

[22] R. Racke and S. Zheng, Adv. Differ. Equ. **8**, 83 (2003).